Volume 1 | Number 1 | Jan 2013 | Pages 1–100

PCCP

Physical Chemistry Chemical Physics
www.rsc.org/pccp

ROYAL SOCIETY OF CHEMISTRY

ROYAL SOCIETY OF CHEMISTRY

www.rsc.org/pccp

Influence of sumanene modifications with boron and nitrogen atoms to its hydrogen adsorption properties

Stevan Armaković[1], Sanja J. Armaković[2,*], Svetlana Pelemiš[3], Dragoljub Mirjanić[4,5]

[1] University of Novi Sad, Faculty of Sciences, Department of Physics, Trg Dositeja Obradovića 4, 21000, Novi Sad, Serbia,

[2] University of Novi Sad, Faculty of Sciences, Department of Chemistry, Biochemistry and Environmental Protection, Trg Dositeja Obradovića 3, 21000, Novi Sad, Serbia,

[3] University of East Sarajevo, Faculty of Technology, Zvornik, Karakaj bb, 75400 Zvornik, Republic of Srpska, Bosnia and Herzegovina

[4] University of Banja Luka, Medical Faculty, 78000 Banja Luka, Republic of Srpska, Bosnia and Herzegovina

[5] Academy of Sciences and Arts of the Republic of Srpska, Trg srpskih vladara 2, 78000 Banja Luka, Republic of Srpska, Bosnia and Herzegovina

* **Corresponding Author:** Sanja J. Armaković,

Telephone: +381 21 485 2754

E-mail: sanja.armakovic@dh.uns.ac.rs

ABSTRACT: We have investigated the influence of the sumanene modifications to the adsorption properties towards hydrogen molecule. Benzylic positions of sumanene were substituted with boron and nitrogen atoms, which changed its hydrogen storage properties. H_2 binding energies have been calculated with LMP2, DFT and DFT-D3 approaches with several exchange-correlation functionals and the results indicate physisorption mechanism. The physisorption was confirmed by fragment analysis and a special attention was paid to the non-covalent interactions. All non-covalent interactions, based on reduced density gradient surfaces, have been identified and calculated, for better understand of adsorption mechanism. Also the significance of charge separation by inducing boron and nitrogen atoms was emphasized and a special attention was paid to the *z*-component of dipole moment of sumanene derivatives.

KEYWORDS: Sumanene, Hydrogen adsorption, Physisorption, Reduced density gradient (RDG), Non-covalent interactions, Fragment analysis

1. Introduction

For decades mankind is devoted to finding the appropriate way to replace the usage of harmful fossil fuels with hydrogen, since hydrogen is considered as a pure energy carrier [1, 2]. By many criteria hydrogen is a future alternative energetic resource [3]. In contrast to the environmental advantages of hydrogen over fossil fuels, a major drawback of hydrogen is related to its efficiency in relation to the volume which is very low [4]. This drawback leads to the need to implement the high pressure and cryogenic storage methods, which are not suitable in terms of practicality. Namely, these techniques have not been perfected yet to be considered safe [4].

Therefore, one of the main goals of scientific community is to find appropriate hydrogen storage media. In that sense the nanomaterials based on carbon, such as carbon nanotubes, graphenes and fullerenes have a significant attention of research teams due to many reasons. Mentioned nanostructures possess different properties that are important for hydrogen storage, among which are high surface area, light weight, suitable pore structure, availability, etc [5-8]. The positive side of carbon structures is the fact that the adsorption of hydrogen is based on the physisorption mechanism, enabling efficiently both the adsorption and desorption of hydrogen under ambient conditions [9-11].

Many studies are also related to the various modifications and functionalization of carbon nanostructures in order to improve the hydrogen binding energies. In this regard, the substitution with atoms (hetero, alkali or rare earths), introduction of defects and functionalization with other molecules have been suggested [1, 5, 8, 12-18].

The hydrogen storage potential of bowl-shaped π-conjugated compounds (or simply π-bowls) is yet to be explored in a significant extent. The adsorption properties of π-bowls based on the physisorption might be of a great importance for the future energy solutions based on "clean" technologies. There are several reasons why the π-bowls should be considered as potential hydrogen storage mediums. Due to the bowl shaped geometry π-bowls have two surfaces (concave and convex) with different adsorption properties [19-21]. Another consequence of the bowl shaped geometry is that the more negative charge located on the concave side leads to intensive charge separation, which is crucial for the adsorption based on electrostatic interaction

[22-24]. Finally, the π-bowls are readily modified, especially if they possess the so called benzylic positions, such as in the case of sumanene molecule [25].

Typical representatives of this group of molecules are corannulene and sumanene, which could be considered as fullerene fragments, Figure 1. Corannulene, the first typical representative of the π-bowls, was successfully synthetized by Barth and Lawton in 1966 [26]. Consequently, most of the attention has been focused to this C_{5v} symmetric molecule. C_{3v} symmetrical sumanene was successfully synthetized under mild conditions almost forty years after the corannulene, in 2003. by Sakurai et al. [27].
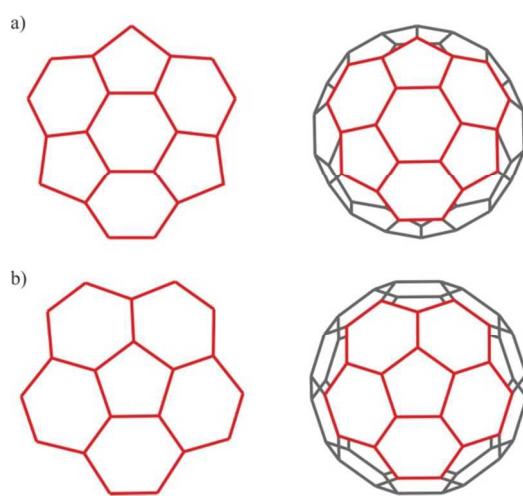
Figure 1. Structures of a) sumanene and b) corannulene
considered as fullerene fragments

The C_{3v} symmetric sumanene molecule has certain advantages over corannulene, thus this molecule has drawn significant attention by both theorists and experimentalists. It has higher bowl depth, charge separation is also higher and from the aspect of functionalization it is important to emphasize the fact that it has three sp^3 hybridized carbon atoms at the benzylic positions, which allows further functionalization of a new bowl shaped structures [25, 28].

We have recently shown, from the aspect of density functional theory (DFT) calculations, that sumanene may be an interesting candidate as an efficient hydrogen storage medium [22]. In the present work we have focused on the adsorption properties of sumanene derivatives obtained after the substitution of benzylic carbon atoms with B and N atoms. These derivatives were in our focus as well; in two recent publications we investigated them in details [24, 29]. Motivation

for the research of adsorption properties of mentioned derivatives we find in the fact that they possess a significant charge separation, which is prerequisite for positive adsorption properties towards hydrogen. Besides, it is well known that B and N are common dopants for carbonaceous materials [30].

Several studies might be important for the achievement of modifications of sumanene with B and N atoms. Namely, Wang et al [31] investigated the decomposition process of carbon-containing molecules, namely the ethene, on Rh(111) surface following the temperature-programmed growth (TPG) method. Thanks to the scanning tunneling microscopy (STM) and DFT calculations they have determined that TPG leads to the synthesis of graphene nano-islands whose size is of several hundreds of nanometers. It was also concluded that carbon nano-islands possess honeycomb structure consisting of seven fused benzene rings, denoted as 7-C6. The hydrogenated version of 7-C6 is precisely the coronene molecule, a planar relative of buckybowls. Similarly, Cui et al. [32] have shown that graphene nanoclusters of identical sizes form on Ru(0001). Two types of graphene nanoclusters are identified and one of them is again 7-C6 while the other graphene nanocluster consists of three fused benzene rings and is denoted as 3-C6. These findings were followed by adequate theoretical studies [33-35] that gave an important insights related to structures and stabilities of the mentioned nanoclusters, while all of these studies may play crucial role when it comes to the modifications of structures such as buckybowls.

Interactions between carbon based structures and hydrogen molecules are of non-covalent nature, thus the choice of theoretical approach is crucial for obtaining valid results. Following the recommendations of Zhao and Truhlar in their papers [36-42], we decided to use primarily the M06-2X functional for the investigation of H_2 adsorption properties of sumanene. It was shown by several benchmark studies that M06 based functionals provide better performance than MP2 approach over broad range of properties [36-48]. Zhao and Truhlar [38] have shown that the mean unsigned error (MUE) of MP2 is three times higher than the MUE of M06-2X functional. In the same time LMP2 was tested against modern M06 based functionals and it was determined that for example precisely M06-2X has similar or even better performance than LMP2 [43].

According to literature data analyzed for this study, we determined that DFT approach with PBE, PW91 and B3LYP-D functionals, together with MP2 approach, have been used for

investigation of H_2 adsorption by other carbon based structures such as carbon nanotubes and graphenes. In order to make our results more reliable we decided to run calculations within localized MP2 (LMP2) [49, 50], DFT and DFT-D3 approach with various functionals.

2. Computational details

DFT calculations of systems sumanene derivative + H_2 were done with Jaguar program 8.8. [43], as implemented in Schrödinger Materials Science 2015-2 suite of programs [51]. Geometrical optimizations were performed within LMP2 [49, 50], DFT and DFT-D3 [52, 53] approaches with different exchange-correlation functionals, namely M06-2X [37], M06-2X-D3, PBE [54, 55], PBE-D3, B3LYP-D3, [36, 37] and with 6-31+G(d,p) basis set. LMP2 level of theory with the different basis sets have been employed in order to optimize geometry of pristine sumanene + H_2 so comparison with other works could be done. Selection of the used functionals is discussed later. For obtaining equilibrium geometries we used settings better than default. Namely, the grid density for DFT calculations was set to fine instead of medium, while accuracy of calculations was set to accurate. The self-consistent field energy cut off was set to 5×10^{-5} a.u while the direct inversion in the iterative subspace (DIIS) convergence scheme was used. Information on dipole moments of investigated derivatives were taken from our previous works [24, 29]. Both the parallel and normal initial orientations of H_2 molecules have been tried.

The main adsorption property, the H_2 binding energy, was calculated according to the following equation:

$$E_B = E_{\text{Sumanene derivative} + H_2} - E_{\text{Sumanene derivative}} - E_{H_2} \qquad (1)$$

In the equation (1) $E_{\text{Sumanene derivative} + H_2}$ stands for total energy of system sumanene derivative + H_2, $E_{\text{Sumanene derivative}}$ denotes total energy of sumanene derivative, while E_{H_2} stands for total energy of H_2 molecule. In order to take into account the basis set superposition error (BSSE), the counterpoise correction by Boyse and Bernardi was included [56].

Analysis based on the reduced density gradient (RDG) was used in order to identify and quantify the nature of non-covalent interactions. Such approach based on electron density and its reduced gradients was recently introduced by Yang et al. [57-59]. In order to investigate the adsorption mechanism in details a fragment analysis as implemented in Amsterdam Density Functional (ADF) Molecular Modeling Suite has been performed employing the dispersion corrected PBE-D3(BJ) functional [52-54] with ATZ2P basis set.

3. Results and Discussions

3.1. Binding energies

We will begin the discussion of results by comparing the H_2 binding energies of sumanene and corannulene because, to the best of our knowledge, only these two representatives of buckybowls have been investigated for H_2 adsorption properties. Table 1 contains information on the H_2 binding energies for corannulene taken from corresponding studies with MP2 approach and for sumanene as calculated in our herein presented study with LMP2 approach.

Table 1. Comparison of H_2 binding energy of sumanene and corannulene

adsorption side/adsorption mode	Sumanene + H_2 binding energies [kcal/mol]		Corannulene + H_2 binding energies [kcal/mol]
	cnv/para	cnv/norm	cnv/norm
(L)MP2/6-31Gd	−0.44[a]	−0.48[a]	−0.32[b] −0.91[c] −0.94[d]
LMP2/6-31G(d,p)	−0.63[a]	−0.65[a]	no literature data
LMP2/6-31+G(d,p)	−0.96[a]	−1.07[a]	no literature data

cnv=concave, cnvx=convex, norm=normal, para=parallel; a) This work, H_2 adsorption from concave side only, b) Reference [60]; with BSSE correction, c) Reference [60]; without BSSE correction, d) Reference [9]; without BSSE correction

Corannulene has been investigated for H_2 adsorption properties by Scannlon et al. [9] and Reisi-Vanani et al. [60, 61]. In both studies MP2 approach has been employed and it has been shown that the adsorption of hydrogen in normal orientation with regard to the central ring of corannulene is more stable than parallel orientation.

Scanlon et al. reported two set of values for H_2 binding energies of corannulene. The first one, −0.82 and −0.91 kcal/mol, corresponds to the adsorption from convex and concave side as calculated at MP2/6-31G(d) level of theory. The second set of values, −1.38 and −2.82 kcal/mol corresponds again to the H_2 adsorption from convex and concave side respectively, calculated by single point energy calculation at MP2(Full)/6-311++G(3df,2p) level of theory using geometries obtained at MP2/6-31G(d) level of theory. In the same study of corannulene Scanlon et al. [9] calculated weight percent for the case of one adsorbed hydrogen molecule to be 0.79 % wt. Due to the very similar chemical formulas, weight percent for the case of one adsorbed hydrogen molecule by sumanene is very similar, 0.76 wt %. However, hydrogen capacity of sumanene can be discussed only after detailed investigation at molecular dynamics level.

Their subsequent study of corannulene complexed with lithium atoms showed that the H_2 binding energies of corannulene may increase from −0.92 kcal/mol to −2.82 kcal/mol [10]. Corannulene and its derivatives with two N atoms were investigated by Reisi-Vanani and Alihoseini [60] at MP2/6-31G(d) level of theory. They have concluded that modifications with N atoms improve the adsorption properties of corannulene, while the binding energies with BSSE correction for adsorption from concave side ranged from −0.32 kcal/mol, for pristine corannulene, to −0.45 kcal/mol for one derivative.

Our study with LMP2 approach and the same basis set as in works where corannulene was investigated indicate somewhat higher H_2 binding energy and the same fact that normal orientation of H_2 molecule leads to the more stable adsorption. Study of Scanlon et al. showed that significantly higher adsorption energy is obtained when larger basis set is used, so we decided to check LMP2 approach with two more basis sets, 6-31G(d,p) and 6-31+G(d,p), with full geometrical optimizations (Table 1). As in the case of Scanlon et al. [9], larger basis set led to the significantly higher H_2 binding energies.

On the other side employment of DFT approach and different functionals led to different results, not only when it comes to the magnitude of H_2 binding energies, but also when it comes to the question which H_2 orientation leads to the more stable adsorption. H_2 binding energies calculated with different functionals, regular and dispersion-corrected, are presented in Table 2.

Table 2. H$_2$ binding energy of sumanene calculated with different functionals and 6-31+G(d,p) basis set

Functionals	Binding energies [kcal/mol]	
	para	norm
M06-2X	−3.25	−2.86
M06-2X-D3	−3.42	−3.05
PBE	−0.32	−0.22
PBE-D3	−2.45	−2.26
B3LYP-D3	−2.37	−2.18

The results in Table 2 indicate in all cases that the parallel orientation of H$_2$ molecule is more favored when it comes to the adsorption by sumanene molecule. In all cases DFT approach also predicts significantly stronger binding of H$_2$ to sumanene than LMP2 approach, osim u slucaju PBE. This is however changed when dispersion-corrected version of PBE is used (Table 3). Table 3 contains information on binding energies of sumanene modified with B and N atoms, as calculated with different functionals. Sumanene derivatives with different number of B or N atoms are denoted as Sum/nB(N), where n is the number of substituted atoms.

Table 3. H$_2$ binding energies of sumanene derivatives in [kcal/mol] with different functionals and 6-31+G(d,p) basis set and counterpoise correction included

System	M06-2X		M06-2X-D3		PBE		PBE-D3		B3LYP-D3	
H$_2$ orientation	para	norm	para	norm	para	norm	para	norm	para	norm
Sumanene+H$_2$	−3.25	−2.86	−3.42	−3.05	−0.32	−0.22	−2.45	−2.26	−2.37	−2.18
Sum/1B+H$_2$	−3.10	−2.75	−3.27	−2.94	−0.32	−0.18	−2.42	−2.20	−2.30	−2.13
Sum/1N+H$_2$	−3.42	−3.03	−3.59	−3.22	−0.31	−0.18	−2.49	−2.30	−2.41	−2.23
Sum/2B+H$_2$	−2.88	−2.61	−3.05	−2.80	−0.32	−0.19	−2.32	−2.14	−2.18	−2.06
Sum/2N+H$_2$	−3.65	−3.20	−3.81	−3.37	−0.32	−0.19	−2.58	−2.32	−2.55	−2.27
Sum/3B+H$_2$	−2.61	−2.45	−2.79	−2.64	−0.29	−0.19	−2.17	−2.06	−2.01	−1.98
Sum/3N+H$_2$	−3.80	−3.36	−3.94	−3.55	−0.26	−0.21	−2.58	−2.37	−2.57	−2.33

The parallel orientation of H$_2$ molecule is favored in all cases. Modifications with B atoms decrease the H$_2$ binding energy, while modifications with N atoms increase the H$_2$ binding energies. This trend is not followed only in the case of PBE functional, which is not strange taking into account the position of this functional on the hierarchical ladder of functionals. Dispersion corrected functionals provide significantly improved results, providing very good

alternative for computationally expensive (L)MP2 approach. Geometries obtained with M06-2X functional and 6-31+G(d,p) basis set are presented in Figure 2.
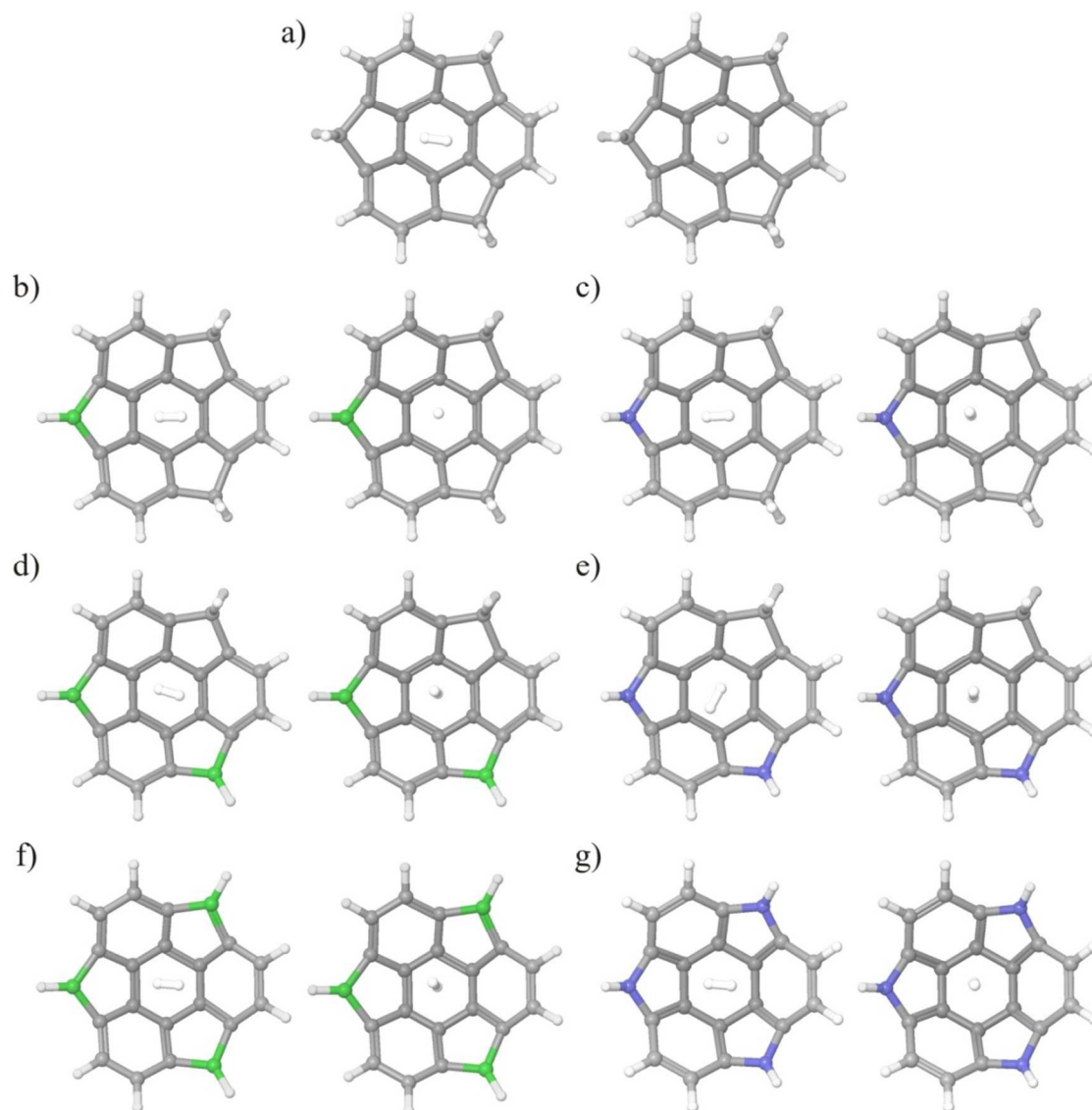
Figure 2. Equilibrium geometries of pristine and modified sumanene with the adsorbed H_2 molecule. Left side corresponds to parallel and right to normal orientation of adsorbed H_2 molecule. Green color corresponds to B while blue corresponds to N atoms

The results presented in Table 3 emphasize the potential of sumanene to be applied in the practical solutions involving H_2 as a fuel of the future. The binding energy of pristine sumanene

in this study is calculated to be -3.25 kcal/mol. We have to note that obtained H_2 binding energy for pristine sumanene significantly differs from the value obtained in our previous work [22], which was -0.32 kcal/mol. This is not strange since in our previous initial study we used B3LYP functional.

Obtained H_2 binding energy for pristine sumanene is very competitive with the results obtained of other nanostructures which can be considered as popular, when it comes to the research of hydrogen adsorption properties. Probably the most popular carbon based nanostructures for the investigation of adsorption properties towards hydrogen molecules are graphene and carbon nanotubes. Arellano et al. [62] investigated the interactions between hydrogen and (5,5) and (6,6) single-wall carbon nanotubes within LDA approach. They stated that outside the nanotube H_2 binding energy was ranging from 0.92 to 1.61 kcal/mol. Consequently they concluded that the uptake and release of molecular hydrogen from nanotubes is a relatively easy process, which is of a great importance for practical applications.

Henwood and Carey have investigated the molecular hydrogen physisorption on graphene and carbon nanotubes [63], applying periodic DFT approach with both LDA and GGA approximations. Depending on the binding sites, the H_2 binding energies for graphene in their study were calculated to be in the range of 1.75 kcal/mol to 2.14 kcal/mol when the LDA approximation was applied, while for GGA approximation binding energies were somewhat lower and were in the range of 0.51 kcal/mol to 0.55 kcal/mol. It is also known fact that LDA functional tends to overestimate, while GGA tends to underestimate binding energies [63]. Concerning the H_2 binding energies of (9,0) and (10,0) carbon nanotubes, they were in the range of 1.45 kcal/mol to 2.10 kcal for LDA functional and in the range of 0.46 kcal/mol to 0.52 kcal/mol for GGA functional.

In order to improve H_2 adsorption properties, many techniques and approaches have been suggested. Therefore, the different types of decorations, modifications and functionalization of carbon based structures have been modeled and the adsorption properties were tested. Related to this Seenithurai et al. [4] investigated the effects of Al atom substitution into the structure of (8,0) carbon nanotube towards the H_2 adsorption properties within LDA approach and with Perdew-Wang (PW) correlation. Beside the fact that Al atoms increase the average H_2 binding energy to 4.93 kcal/mol, they also increase the capacity of nanostructure since each Al atom could adsorb four H_2 molecules. They also cited the important results of two papers in which the

LDA approach was compared with MP2 method. Namely, Okamoto and Miyamoto [64] have shown that LDA results obtained for H_2 physisorption on carbon nanostructures are in good agreement with the results obtained by MP2 approach, while Ao et al. [65] calculated the difference in the obtained binding energies between LDA and MP2 to be 6%, for Al-doped graphene.

The different types of nanosheets and nanotubes, their analogues, have been also considered for the adsorption of H_2. For example Moradi and Naderi conducted investigation of H_2 adsorption properties of graphene analogue – aluminum nitride nanosheet using empirically corrected B3LYP functional, namely the B3LYP-D [66]. Their calculations indicated that AlN nanosheet can adsorb the H_2 molecule with binding energies of −1.9 and −5.2 kcal/mol, depending on binding sites. On the other side Zhou et al. [67] compared H_2 adsorption properties of carbon and boron-nitride (BN) nanotubes. Using PW91 functional for (9,0) carbon and BN nanotube they calculated the H_2 adsorption energies to be −0.63 kcal/mol and −0.30 kcal/mol, respectively. With PBE functional they obtained much lower adsorption energies, −0.40 and −0.08 kcal/mol, for carbon and BN nanotubes respectively. This is of course in agreement with the known fact about the PBE and vdW interactions, while the conclusion from their work was that CNTs adsorb H_2 molecules with higher binding energy than BNNTs.

Taking into account the result obtained for pristine sumanene, for which the H_2 binding energy is calculated to be −3.25 kcal/mol, it can be concluded that this interesting molecule has excellent adsorption properties towards the H_2 molecule, leaving enough space to be improved with modifications, for example with B and N atoms.

As expected and shown in our previous publications [24, 29], the introduction of B and N atoms induced significant changes to the electronic system of sumanene. This has also reflected to the H_2 adsorption properties, which significantly reduced in the case when B atoms were introduced, while a significant improvement happened when N atoms were introduced. Both the reduction and improvement of the H_2 adsorption properties happened subsequently with the number of introduced atoms. In the case of derivatives with B atoms, the H_2 binding energies decreased from −3.25 kcal/mol (for pristine sumanene) to −3.10, −2.88 and −2.61 kcal/mol for derivatives containing one, two and three B atoms, respectively. The opposite situation happened when N atoms were introduced, namely H_2 binding energies increased to −3.42, −3.65 and −3.80 kcal/mol for derivatives containing one, two and three N atoms, respectively.

Beside H_2 binding energies, another important parameter related to the practical application of sumanene for hydrogen storage is certainly the storage limit. For example, in their study of corannulene hydrogen storage Scanlon et al. [9] calculated weight percent for the case of one adsorbed hydrogen molecule to be 0.79 % wt. Due to the very similar chemical formulas, weight percent for the case of one adsorbed hydrogen molecule by sumanene is very similar, 0.76 wt %. In our study we also tested the hydrogen uptake from concave side of sumanene and its B and N derivatives at B3LYP-D3/6-31G(d) level of theory. We used this level of theory because it is much more computationally affordable than M06-2X/6-31+G(d,p), while in the same time the results in Table 3 indicate excellent performance of this empirically corrected exchange-correlation functional. Using this level of theory geometrical optimization successfully yielded molecular configurations with two and three H_2 molecules above sumanene and its B and N derivatives from concave side. This means that sumanene molecule and its B and N derivatives are able to accommodate at least three H_2 molecules from concave side and the weight percent ranges from 2.24 % wt (for sumanene derivative with three N atoms) to 2.32 % wt (for sumanene derivative with three B atoms).

Before we further discuss the obtained results, in the following section we will shortly refer to the adsorption mechanism.

3.2. Adsorption mechanism

Although the calculated binding energies may indicate the physisorption mechanism based on electrostatic interaction, because there are no studies on the adsorption properties of sumanene nor its derivatives, the introduction of B and N atoms impose the task of adsorption mechanism determination. For these purposes the fragment analysis as implemented in ADF 2014.2 molecular modeling suite might be of particular interest. This approach offers the ability to determine the percentage contribution of molecular orbitals of user defined fragments to the frontier molecular orbitals of the whole system and thus determines the overall influence of the defined fragment. The fragment analysis in ADF is based on the symmetrized fragment orbitals (SFO) and herein we will not deal with the details about this approach for the sake of simplicity, while important details about this approach can be found in the reference by te Velde et al. [68].

Taking into account the fragment approach in ADF, the system consisting of sumanene derivative + H_2 molecule is divided in two fragments. One fragment is the sumanene derivative and the other fragment is the H_2 molecule. After the fragment analysis is conducted at the PBE-D3(BJ)/ATZ2P level of theory, the percentage contribution of molecular orbitals of defined fragments to the frontier molecular orbitals of the whole system is obtained. This information is provided in Table 4.

Table 4. Fragment analysis of frontier orbital contributions

| System | Contribution of fragment SFO to the frontier MO's [%] | | | |
| | Fragment 1.Sumanenederivative | | Fragment 2. H_2 | |
	HOMO	LUMO	HOMO	LUMO
Sum/1B+H_2	99.88	99.46	0.06	0.18
Sum/1N+H_2	99.50	99.92	0.47	0.06
Sum/2B+H_2	99.93	99.44	0.03	0.34
Sum/2N+H_2	100.00	99.41	0.00	0.37
Sum/3B+H_2	100.00	99.44	0.00	0.42
Sum/3N+H_2	99.83	99.72	0.12	0.16

It should be noted that SFOs are linear combinations of (valence) Fragment Orbitals (FOs) and that only first members are presented in the output. The results of fragment analysis in ADF can be also presented in the form of energy levels. For the sake of clarity we are providing these results in the supplementary information, Figures S1-S4, because the all orbital levels are very similar in terms of fragment contribution to frontier orbitals, while in Figure 3 we provide the energy levels of fragment analysis for the cases of H_2 adsorption by sumanene derivatives with three B and N atoms.
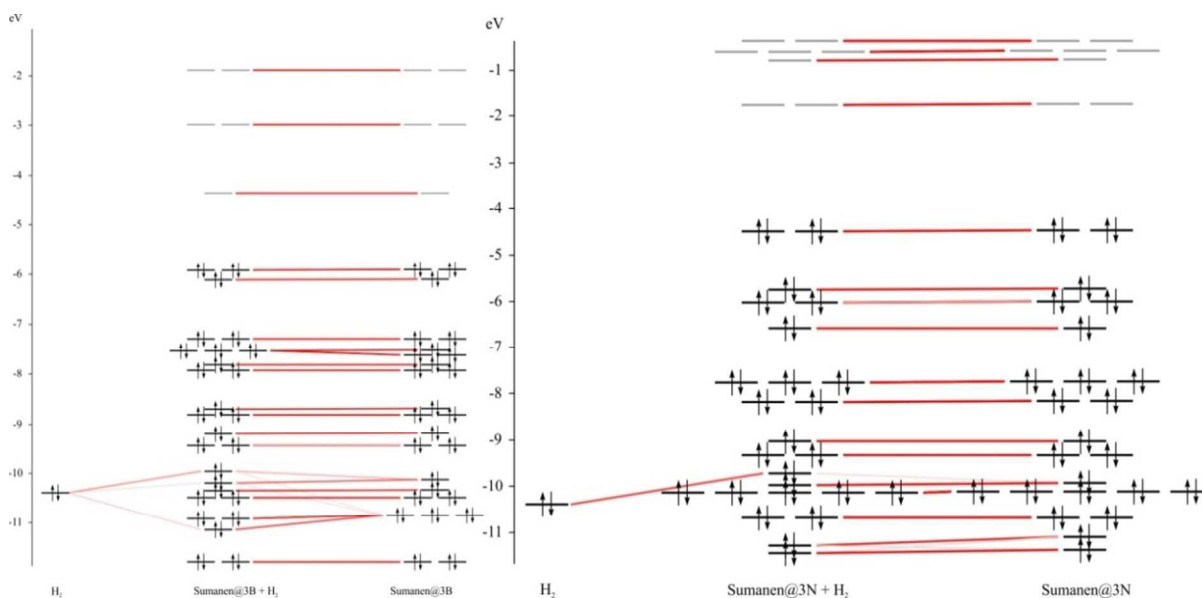
Figure 3. Energy levels of fragment analysis for the cases of H_2 adsorption by sumanene derivatives with three a) B and b) N atoms

In Figure 3 the interactions of fragments are presented with red lines. Clearly, one can see that H_2 contribution is far away from frontier orbitals, while all significant contribution comes from sumanene derivatives. After the inspection of conducted fragment analysis it can be concluded that the contribution of H_2 fragment to frontier orbitals is negligible in comparison with contribution of sumanene derivatives. This clearly confirms the physisorption mechanism of H_2 on sumanene modified with B and N atoms. It is also important to emphasize that the physisorption mechanism is responsible for adsorption of CO, CO_2 and NH_3 molecules by sumanene, as shown in our previous study [23].

The fact that the physisorption occurs between sumanene derivatives and H_2 molecules is of a great importance from the aspect of practical applicability. Although physisorption provides binding energies that are much lower than the binding energies in case of chemisorption, in the same time it enables both the adsorption and desorption under ambient temperatures. The chemisorption on the other side enables better binding of H_2 to adsorbent, but in such case much higher temperatures are needed in order to break the bond between H_2 and adsorbent, in order to use the H_2 [10]. For example, when metal hydrides are used for hydrogen adsorption, the chemisorption is principally responsible for the interaction, while the efficient desorption of

hydrogen occurs at temperatures above 500 K with the low uptake capacity in the same time [10, 69-72].

Since the non-covalent interactions are responsible for interesting adsorption properties of sumanene, in the next chapter we are presenting results concerning the detailed investigation of non-covalent interactions.

3.3. Non-covalent interactions

The results presented in the previous chapter clearly indicate that non-covalent interactions are principally responsible for positive H_2 adsorption properties of sumanene derivatives investigated in this work. Therefore, applying the non-covalent interactions module of Jaguar program, we decided to determine those interactions. A method of Johnston et al. [73, 74] could be particularly useful in order to visualize the non-covalent interactions between the sumanene derivatives and H_2 molecules. It is a convenient way to obtain the surface map in which isosurfaces indicate the interactions between non-covalently bounded atoms. Colors of map determine the strength, favorability and un-favorability of the interactions [75]. RDG surfaces and non-covalent interactions that occur between sumanene derivatives and H_2 molecules are presented in Figure 4 and 5.

In Figure 4 and 5, significant RDG surface areas and non-covalent interactions between sumanene derivatives and H_2 molecules are visible above the central six member (hub) ring of sumanene, in all cases. The purpose of RDG surfaces presented in Figure 4 and 5 was to emphasize the importance of area above central ring od sumanene, bearing in mind the fact that the more negative charge is located at the concave side of buckybowls, which is the consequence of specific bowl shaped geometry [22-24, 29]. Since the surfaces of buckybowls are differently charged, this also results in dipole moment which is principally responsible for adsorption of otherwise non-polar molecules. One can see that all non-covalent interactions occur between H_2 molecule on one side and carbon atoms belonging to hub ring on the other side. On the other side, the number of non-covalent interactions between B and N sumanene derivatives varies between one and three. One can see that all non-covalent interactions occur between H_2 molecule on one side and carbon atoms belonging to hub ring on the other side. On the other side, the

number of non-covalent interactions between B and N sumanene derivatives varies between one and three.
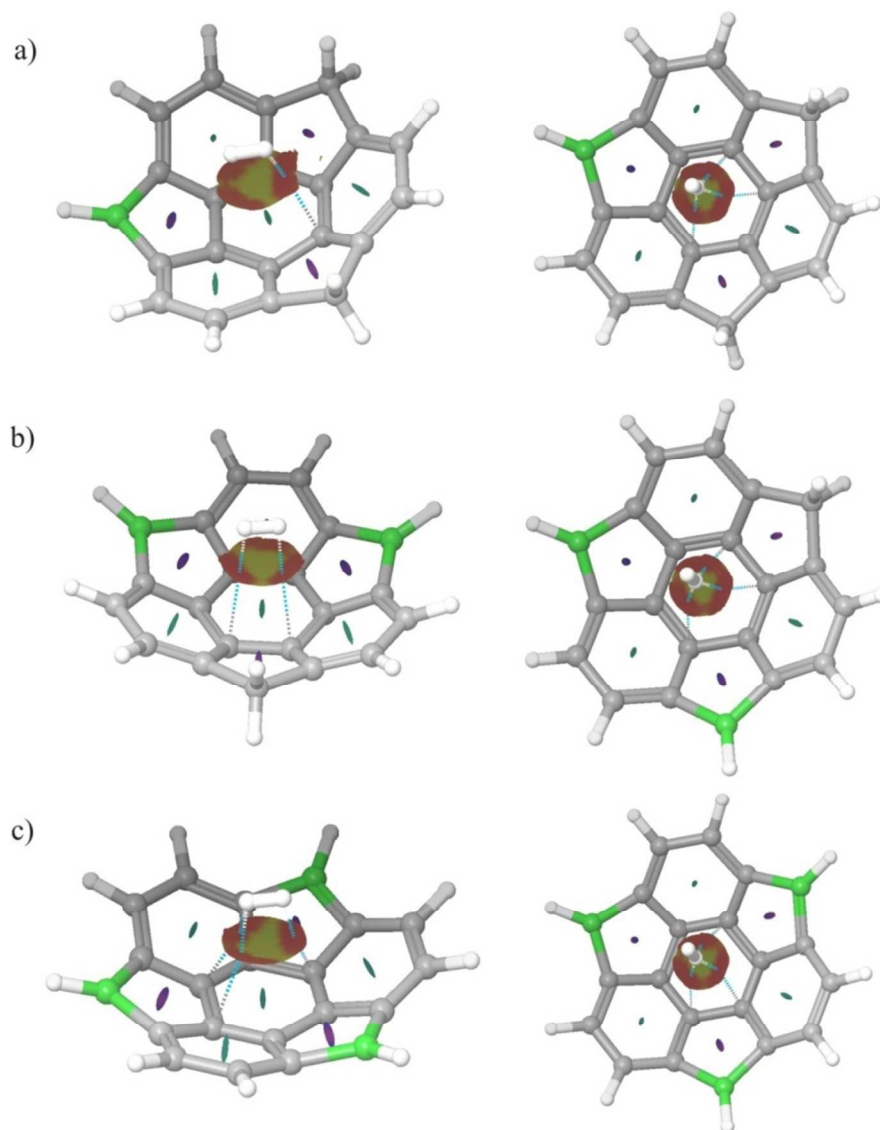
Figure 4. RDG surfaces with indicated non-covalent interactions (dashed lines) between sumanene derivatives with a) one, b) two and c) three B atoms. Left side corresponds to parallel and right to normal orientation of adsorbed H_2 molecule.
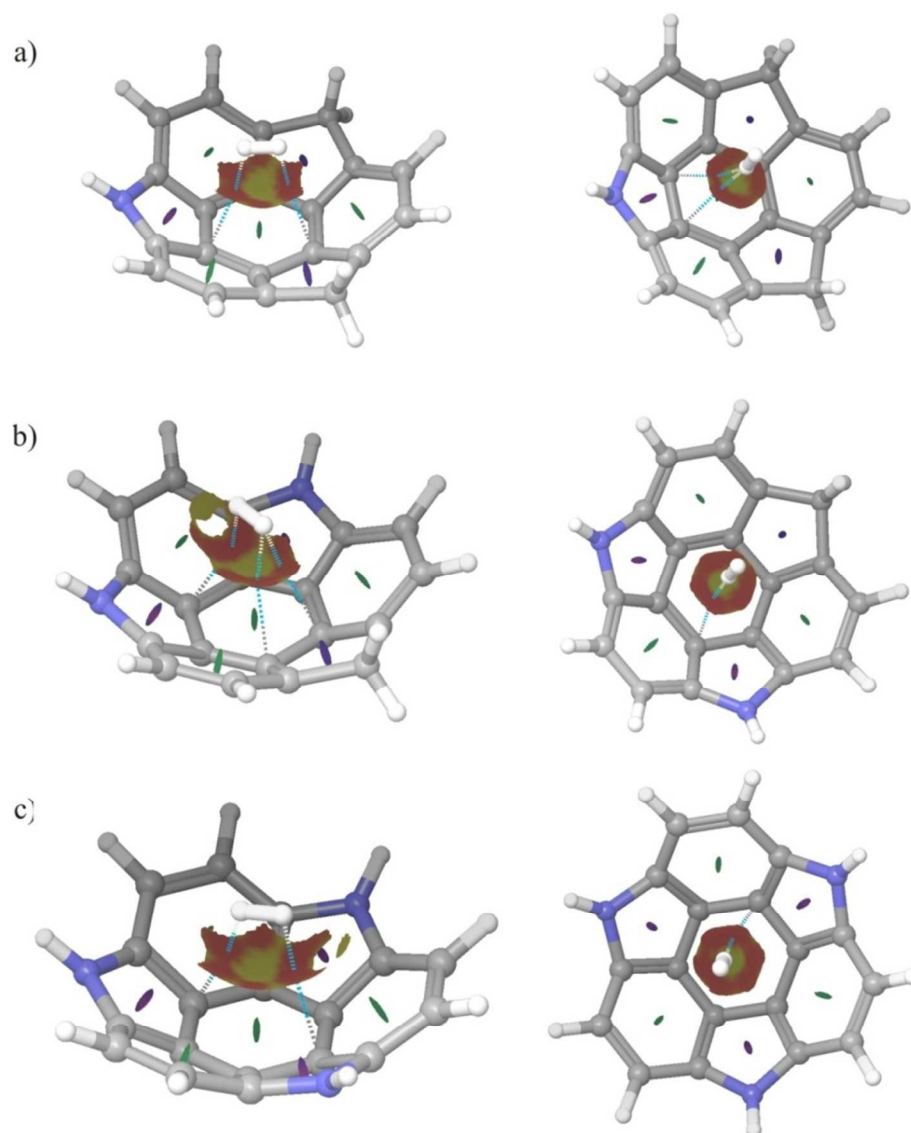
Figure 5. RDG surfaces with indicated non-covalent interactions (dashed lines) between sumanene derivatives with a) one, b) two and c) three N atoms. Left side corresponds to parallel and right to normal orientation of adsorbed H_2 molecule.

Concerning the sumanene derivatives with B atoms, the number of non-covalent interactions increases from one to three subsequently with the increase of the number of B atoms, for the case when the adsorbed H_2 molecule is in parallel orientation. When H_2 molecule is in normal orientation the number of non-covalent interactions is always three. On the other side, the number of non-covalent interactions for the case of sumanene derivatives with N atoms is never less than two for the case of parallel orientation of H_2 molecule, while for the case of normal

orientation of H_2 molecule number of non-covalent interactions is never higher than two. The visualization of non-covalent interactions may provide the answer to question why is the parallel orientation of adsorbed H_2 molecule more favored than normal orientation. Namely, it can be seen clearly from Figures 4 and 5 that for parallel orientation both H_2 atoms participate in non-covalent interactions, except for the case of sumanene derivative with one B atom (but nevertheless, for this and the rest of cases RDG surface is larger for parallel than for normal orientation). Contrary to this, when H_2 molecules are in normal orientation there is always only one hydrogen atom that participate in non-covalent interactions.

3.4. Dipole moments – the role of charge separation

Although modifications with B and N atoms of different carbonaceous materials have led to the improvement their various properties, with sumanene happened significant difference when it comes to the H_2 adsorption properties. Namely, results presented in the section 3.1. indicate significantly higher H_2 binding energies for derivatives containing N atoms. Obtained H_2 binding energies and the difference in H_2 adsorption properties between derivatives modified with B and N atoms could be explained by the detailed inspection of dipole moments, Table 5. In the mentioned table derivatives with certain number of B and N atoms are denoted as Sumanene/nB(N).

Speaking of van der Waals interactions it is important to note that hydrogen molecule does not have permanent dipole moment. This imposes the necessity of the adsorbent having relatively high dipole moment in order that physisorption happen. This criteria is fulfilled in the case of sumanene, which has the dipole moment of 1.96 D, as calculated in our previous works [22, 23, 29]. The relatively high dipole moment of sumanene is able to induce the dipole moment in H_2 molecule and make the physisorption possible. Sumanene has higher dipole moment than corannulene (at B3LYP/6-31Gd level of theory for corannulene we have calculated value of 1.71 D for dipole moment), so that is the reason why it adsorbs H_2 molecules with higher binding energies.

Table 5. Total dipole moments and its components for sumanene and its derivatives with H_2 binding energies calculated at M06-2X/6-31+G(d,p) level of theory

System	Dipole moment[a] [D]	x-component[a] [D]	y-component[a] [D]	z-component[a] [D]	H_2 binding energy[b] [kcal/mol]
Sumanene	1.96	0.00	0.00	1.96	–3.25
Sum/1B	2.54	0.00	1.93	1.64	–3.10
Sum/1N	2.98	0.00	0.73	2.88	–3.42
Sum/2B	2.39	1.97	0.00	1.36	–2.88
Sum/2N	3.97	0.90	0.01	3.87	–3.65
Sum/3B	1.12	0.00	0.00	1.12	–2.61
Sum/3N	4.87	0.00	0.00	4.87	–3.80

a) Data taken from our previous works [24, 29] b) Data from this study

Total dipole moments of sumanene derivatives with B and N atoms might lead to the conclusion that the binding energy of both types of derivatives towards H_2 molecules should be better than for pristine sumanene. However, the H_2 binding energies decrease in the case of derivatives with B atoms, subsequently with the increase of number of introduced atoms.

However, a closer inspection of Figure 2 shows that H_2 molecules are being adsorbed along the bowl depth of sumanene, which in our simulations corresponds to z-axis. Therefore, one should look for the values of z-components of dipole moment. The z-component of dipole moment of investigated derivatives finely correlates with the calculated H_2 binding energies.

So, even though total dipole moment of derivatives with one and two B atoms increase, comparing with pristine sumanene, the z-component of dipole moment of these derivatives decreases below the value of z-component of pristine sumanene dipole moment. Thus, the interaction between B derivatives of sumanene and H_2 molecules is weaker than interaction between pristine sumanene and H_2 molecule. On the other side, both the total dipole moment and its z-components increase in the cases of N sumanene derivatives, leading to stronger interaction between these derivatives and H_2 molecules. This analysis explains the improved H_2 adsorption properties of sumanene modified with N atoms.

4. Conclusions

Employing LMP2, DFT and DFT-D3 approaches we have investigated the H_2 adsorption properties of sumanene and its derivatives obtained by substitution of benzylic carbon atom with

B and N atoms. Various relevant functionals have been tested in order to validate obtained results, while the obtained results have been compared with other studies. We have calculated H_2 binding energies, for which it was shown that decrease in the case of derivatives with B atoms, and increase in the case of derivatives with N atoms. H_2 adsorption properties of pristine sumanene have been calculated with LMP2 approach as well, so it could be compared with the results obtained for corannulene in other studies. DFT and DFT-D3 approaches predict that parallel orientation of H_2 molecule is more favored than normal orientation, contrary to the results of MP2 and LMP2 calculations. Employing fragment analysis, as incorporated in ADF molecular modeling suite, it was confirmed that the physisorption is the mechanism of adsorption that occurs between sumanene derivatives and H_2 molecules. Further, applying the method of Johnston et al. RDG surfaces emphasize the importance of hub ring atoms for H_2 adsorption, while visualization of non-covalent interactions indicated that in the case of parallel oriented H_2 molecules both hydrogen atoms participate in non-covalent interactions, explaining why this orientation leads to the higher H_2 binding energies. Finally, different H_2 adsorption binding energies of derivatives with B and N atoms comparing with pristine sumanene have been explained through detailed inspection of dipole moments. Namely, it is concluded that due to the specific bowl-shaped geometry, the *z*-component of the dipole moment was principally responsible for the values of H_2 binding energies.

5. Acknowledgment

References

1.   Devi, N. and V. Gayathri, *Effect of structural defects on the hydrogen adsorption in promising nanostructures.* Computational Materials Science, 2015. **96**: p. 284-289.
2.   Kuang, A., et al., *Ab initio investigation of the adsorption of atomic and molecular hydrogen on AlN nanotubes.* Applied Surface Science, 2015. **346**: p. 24-32.
3.   Naghshineh, N. and M. Hashemianzadeh, *First-principles study of hydrogen storage on Si atoms decorated C 60.* international journal of hydrogen energy, 2009. **34**(5): p. 2319-2324.
4.   Seenithurai, S., et al., *Al-decorated carbon nanotube as the molecular hydrogen storage medium.* international journal of hydrogen energy, 2014. **39**(23): p. 11990-11998.
5.   Hussain, T., et al., *Calcium doped graphane as a hydrogen storage material.* Applied Physics Letters, 2012. **100**(18): p. 183902.
6.   Reyhani, A., et al., *Hydrogen storage in decorated multiwalled carbon nanotubes by Ca, Co, Fe, Ni, and Pd nanoparticles under ambient conditions.* The Journal of Physical Chemistry C, 2011. **115**(14): p. 6994-7001.
7.   Narehood, D., et al., *Diffusion of H 2 adsorbed on single-walled carbon nanotubes.* Physical Review B, 2003. **67**(20): p. 205409.
8.   Yoon, M., et al., *Calcium as the superior coating metal in functionalization of carbon fullerenes for high-capacity hydrogen storage.* Physical review letters, 2008. **100**(20): p. 206806.
9.   Scanlon, L.G., et al., *Investigation of Corannulene for Molecular Hydrogen Storage via Computational Chemistry and Experimentation.* The Journal of Physical Chemistry B, 2006. **110**(15): p. 7688-7694.
10.   Zhang, Y., et al., *Computational investigation of adsorption of molecular hydrogen on lithium-doped corannulene.* The Journal of Physical Chemistry B, 2006. **110**(45): p. 22532-22541.
11.   Cazorla, C., *The role of density functional theory methods in the prediction of nanostructured gas-adsorbent materials.* Coordination Chemistry Reviews, 2015. **300**: p. 142-163.
12.   Luna, C.R., et al., *Hydrogen Adsorption and Associated Electronic and Magnetic Properties of Rh-decorated (8, 0) CNT Using Density Functional Theory.* The Journal of Physical Chemistry C, 2015.
13.   Srinivasadesikan, V., P. Raghunath, and M. Lin, *Quantum chemical investigation on the role of Li adsorbed on anatase (101) surface nano-materials on the storage of molecular hydrogen.* Journal of molecular modeling, 2015. **21**(6): p. 1-10.
14.   Reimers, W.G., M.A. Baltanás, and M.M. Branda, *CO, CO2 and H2 adsorption on ZnO, CeO2, and ZnO/CeO2 surfaces: DFT simulations.* Journal of molecular modeling, 2014. **20**(6): p. 1-10.
15.   Khosravi, A., et al., *First-principles vdW-DF study on the enhanced hydrogen storage capacity of Pt-adsorbed graphene.* Journal of molecular modeling, 2014. **20**(5): p. 1-7.
16.   Tabtimsai, C., et al., *Density functional investigation of hydrogen gas adsorption on Fe− doped pristine and Stone− Wales defected single− walled carbon nanotubes.* Journal of molecular modeling, 2012. **18**(8): p. 3941-3949.

17.   Kalamse, V., N. Wadnerkar, and A. Chaudhari, *Hydrogen storage in C3Ti complex using quantum chemical methods and molecular dynamics simulations.* Journal of molecular modeling, 2012. **18**(6): p. 2423-2431.

18.   Kaewruksa, B. and V. Ruangpornvisuti, *First principles investigation of oxygen adsorptions on hydrogen–terminated ZnO graphene-like nanosheets.* Journal of molecular modeling, 2012. **18**(4): p. 1447-1454.

19.   Spisak, S.N., et al., *Selective Endo and Exo Binding of Alkali Metals to Corannulene.* Angewandte Chemie International Edition, 2011. **50**(35): p. 8090-8094.

20.   Filatov, A.S., et al., *Bowl-Shaped Polyarenes as Concave–Convex Shape Complementary Hosts for C60-and C70-Fullerenes.* Crystal Growth & Design, 2013. **14**(2): p. 756-762.

21.   Vijay, D., et al., *Where to bind in buckybowls? The dilemma of a metal ion.* Physical chemistry chemical physics, 2012. **14**(9): p. 3057-3065.

22.   Armaković, S., S.J. Armaković, and J.P. Šetrajčić, *Hydrogen storage properties of sumanene.* international journal of hydrogen energy, 2013. **38**(27): p. 12190-12198.

23.   Armaković, S., et al., *Sumanene and its adsorption properties towards CO, CO2 and NH3 molecules.* Journal of molecular modeling, 2014. **20**(4): p. 1-14.

24.   Armaković, S., et al., *Optical and bowl-to-bowl inversion properties of sumanene substituted on its benzylic positions; a DFT/TD-DFT study.* Chemical Physics Letters, 2013. **578**: p. 156-161.

25.   Amaya, T. and T. Hirao, *A molecular bowl sumanene.* Chemical Communications, 2011. **47**(38): p. 10524-10535.

26.   Barth, W.E. and R.G. Lawton, *Dibenzo [ghi, mno] fluoranthene.* Journal of the American Chemical Society, 1966. **88**(2): p. 380-381.

27.   Sakurai, H., T. Daiko, and T. Hirao, *A synthesis of sumanene, a fullerene fragment.* Science, 2003. **301**(5641): p. 1878-1878.

28.   Cauët, E. and D. Jacquemin, *A theoretical spectroscopy investigation of oxosumanenes.* Chemical physics letters, 2012. **519**: p. 49-53.

29.   Armaković, S., et al., *Aromaticity, response, and nonlinear optical properties of sumanene modified with boron and nitrogen atoms.* Journal of molecular modeling, 2014. **20**(12): p. 1-13.

30.   Nath, P., et al., *Ab-initio calculation of electronic and optical properties of nitrogen and boron doped graphene nanosheet.* Carbon, 2014. **73**: p. 275-282.

31.   Wang, B., et al., *Size-selective carbon nanoclusters as precursors to the growth of epitaxial graphene.* Nano letters, 2011. **11**(2): p. 424-430.

32.   Cui, Y., et al., *Formation of identical-size graphene nanoclusters on Ru (0001).* Chemical Communications, 2011. **47**(5): p. 1470-1472.

33.   Gao, J. and F. Ding, *The Structure and Stability of Magic Carbon Clusters Observed in Graphene Chemical Vapor Deposition Growth on Ru (0001) and Rh (111) Surfaces.* Angewandte Chemie International Edition, 2014. **53**(51): p. 14031-14035.

34.   Gao, J. and F. Ding, *First-Principles Phase Diagram of Magic-Sized Carbon Clusters on Ru (0001) and Rh (111) Surfaces.* The Journal of Physical Chemistry C, 2015. **119**(20): p. 11086-11093.

35.   Yuan, Q., et al., *Magic carbon clusters in the chemical vapor deposition growth of graphene.* Journal of the American Chemical Society, 2011. **134**(6): p. 2970-2975.

36. Zhao, Y. and D.G. Truhlar, *Comparative DFT study of van der Waals complexes: rare-gas dimers, alkaline-earth dimers, zinc dimer, and zinc-rare-gas dimers.* The Journal of Physical Chemistry A, 2006. **110**(15): p. 5121-5129.

37. Zhao, Y. and D.G. Truhlar, *The M06 suite of density functionals for main group thermochemistry, thermochemical kinetics, noncovalent interactions, excited states, and transition elements: two new functionals and systematic testing of four M06-class functionals and 12 other functionals.* Theoretical Chemistry Accounts, 2008. **120**(1-3): p. 215-241.

38. Zhao, Y. and D.G. Truhlar, *Density functionals with broad applicability in chemistry.* Accounts of Chemical Research, 2008. **41**(2): p. 157-167.

39. Zhao, Y. and D.G. Truhlar, *Exploring the limit of accuracy of the global hybrid meta density functional for main-group thermochemistry, kinetics, and noncovalent interactions.* Journal of Chemical Theory and Computation, 2008. **4**(11): p. 1849-1868.

40. Zhao, Y. and D.G. Truhlar, *Computational characterization and modeling of buckyball tweezers: density functional study of concave–convex ππ interactions.* Physical Chemistry Chemical Physics, 2008. **10**(19): p. 2813-2818.

41. Zhao, Y. and D.G. Truhlar, *Density functional theory for reaction energies: test of meta and hybrid meta functionals, range-separated functionals, and other high-performance functionals.* Journal of Chemical Theory and Computation, 2011. **7**(3): p. 669-676.

42. Zhao, Y. and D.G. Truhlar, *Applications and validations of the Minnesota density functionals.* Chemical Physics Letters, 2011. **502**(1): p. 1-13.

43. Bochevarov, A.D., et al., *Jaguar: A high‐performance quantum chemistry software program with strengths in life and materials sciences.* International Journal of Quantum Chemistry, 2013. **113**(18): p. 2110-2142.

44. Hemberger, P., et al., *A pass too far: dissociation of internal energy selected paracyclophane cations, theory and experiment.* Physical Chemistry Chemical Physics, 2012. **14**(34): p. 11920-11929.

45. Flick, J.C., et al., *Accurate prediction of noncovalent interaction energies with the effective fragment potential method: Comparison of energy components to symmetry-adapted perturbation theory for the S22 test set.* Journal of Chemical Theory and Computation, 2012. **8**(8): p. 2835-2843.

46. Kang, R., et al., *Assessment of theoretical methods for complexes of gold (I) and gold (III) with unsaturated aliphatic hydrocarbon: which density functional should we choose?* Journal of Chemical Theory and Computation, 2011. **7**(12): p. 4002-4011.

47. Biswal, H.S., et al., *Structure of the Indole− Benzene Dimer Revisited.* The Journal of Physical Chemistry A, 2011. **115**(34): p. 9485-9492.

48. Goerigk, L., H. Kruse, and S. Grimme, *Benchmarking Density Functional Methods against the S66 and S66x8 Datasets for Non‐Covalent Interactions.* ChemPhysChem, 2011. **12**(17): p. 3421-3433.

49. Pulay, P. and S. Saebø, *Orbital-invariant formulation and second-order gradient evaluation in Møller-Plesset perturbation theory.* Theoretica chimica acta, 1986. **69**(5-6): p. 357-368.

50. Saebo, S. and P. Pulay, *Local treatment of electron correlation.* Annual Review of Physical Chemistry, 1993. **44**(1): p. 213-236.

51. *Schrödinger Release 2015-2: Materials Science Suite, Schrödinger, LLC, New York, NY, 2015.* 2015.

52.   Grimme, S., et al., *A consistent and accurate ab initio parametrization of density functional dispersion correction (DFT-D) for the 94 elements H-Pu.* The Journal of chemical physics, 2010. **132**(15): p. 154104.

53.   Grimme, S., S. Ehrlich, and L. Goerigk, *Effect of the damping function in dispersion corrected density functional theory.* Journal of computational chemistry, 2011. **32**(7): p. 1456-1465.

54.   Perdew, J.P., K. Burke, and M. Ernzerhof, *Generalized gradient approximation made simple.* Physical review letters, 1996. **77**(18): p. 3865.

55.   Perdew, J.P., K. Burke, and M. Ernzerhof, *Erratum: Generalized Gradient Approximation Made Simple [Phys. Rev. Lett. 77, 3865 (1996)].* Physical Review Letters, 1997. **78**(7): p. 1396-1396.

56.   Boys, S.F. and F.d. Bernardi, *The calculation of small molecular interactions by the differences of separate total energies. Some procedures with reduced errors.* Molecular Physics, 1970. **19**(4): p. 553-566.

57.   Sandhiya, L. and K. Senthilkumar, *A theoretical probe on the non-covalent interactions of sulfadoxine drug with pi-acceptors.* Journal of Molecular Structure, 2014.

58.   Contreras-García, J., et al., *NCIPLOT: A Program for Plotting Noncovalent Interaction Regions.* Journal of Chemical Theory and Computation, 2011. **7**(3): p. 625-632.

59.   Johnson, E.R., et al., *Revealing Noncovalent Interactions.* Journal of the American Chemical Society, 2010. **132**(18): p. 6498-6506.

60.   Reisi-Vanani, A. and L. Alihoseini, *Computational investigation of the adsorption of molecular hydrogen on the nitrogen-doped corannulene as a carbon nano-structure.* Surface Science, 2014. **621**: p. 146-151.

61.   Reisi-Vanani, A. and S. Faghih, *Computational study of the molecular hydrogen physisorption in some of the corannulene derivatives as a carbon nanostructure.* Journal of Saudi Chemical Society, 2014. **18**(5): p. 666-673.

62.   Arellano, J.S., et al., *Interaction of molecular and atomic hydrogen with (5,5) and (6,6) single-wall carbon nanotubes.* The Journal of Chemical Physics, 2002. **117**(5): p. 2281-2288.

63.   Henwood, D. and J.D. Carey, *Ab initio investigation of molecular hydrogen physisorption on graphene and carbon nanotubes.* Physical Review B, 2007. **75**(24): p. 245413.

64.   Okamoto, Y. and Y. Miyamoto, *Ab initio investigation of physisorption of molecular hydrogen on planar and curved graphenes.* The Journal of Physical Chemistry B, 2001. **105**(17): p. 3470-3474.

65.   Ao, Z. and F. Peeters, *High-capacity hydrogen storage in Al-adsorbed graphene.* Physical Review B, 2010. **81**(20): p. 205406.

66.   Moradi, M. and N. Naderi, *First principle study of hydrogen storage on the graphene-like aluminum nitride nanosheet.* Structural Chemistry, 2014. **25**(4): p. 1289-1296.

67.   Zhou, Z., et al., *Comparative study of hydrogen adsorption on carbon and BN nanotubes.* The Journal of Physical Chemistry B, 2006. **110**(27): p. 13363-13369.

68.   Te Velde, G., et al., *Chemistry with ADF.* Journal of Computational Chemistry, 2001. **22**(9): p. 931-967.

69.   Schüth, F., B. Bogdanović, and M. Felderhoff, *Light metal hydrides and complex hydrides for hydrogen storage.* Chemical communications, 2004(20): p. 2249-2258.

70.   Chao, B. and L. Klebanoff, *Hydrogen storage in interstitial metal hydrides.* For a review of interstitial metal hydrides, see, 2012: p. 109.

71.   Ritter, J.A., et al., *Implementing a hydrogen economy.* Materials Today, 2003. **6**(9): p. 18-23.

72.   Hirscher, M., et al., *Hydrogen storage in sonicated carbon materials.* Applied Physics A, 2001. **72**(2): p. 129-132.

73.   Otero-de-la-Roza, A., E.R. Johnson, and J. Contreras-Garcia, *Revealing non-covalent interactions in solids: NCI plots revisited.* Physical Chemistry Chemical Physics, 2012. **14**(35): p. 12165-12172.

74.   Johnson, E.R., et al., *Revealing noncovalent interactions.* Journal of the American Chemical Society, 2010. **132**(18): p. 6498-6506.

75.   Bochevarov, A.D., et al., *Jaguar: A high-performance quantum chemistry software program with strengths in life and materials sciences.* International Journal of Quantum Chemistry, 2013. **113**(18): p. 2110-2142.